Lanthanide Complex-Based Luminescent Probes for Highly Sensitive Time-Gated Luminescence Detection of Hypochlorous Acid

ARTICLE *in* ANALYTICAL CHEMISTRY · NOVEMBER 2012

Impact Factor: 5.64 · DOI: 10.1021/ac3028189 · Source: PubMed

6 AUTHORS, INCLUDING:

Run Zhang
Macquarie University
28 PUBLICATIONS **401** CITATIONS
SEE PROFILE

Zhiqiang Ye
Dalian University of Technology
64 PUBLICATIONS **1,464** CITATIONS
SEE PROFILE

analytical chemistry

Article

pubs.acs.org/ac

Lanthanide Complex-Based Luminescent Probes for Highly Sensitive Time-Gated Luminescence Detection of Hypochlorous Acid

Yunna Xiao, Run Zhang, Zhiqiang Ye,* Zhichao Dai, Huaying An, and Jingli Yuan*

State Key Laboratory of Fine Chemicals, School of Chemistry, Dalian University of Technology, Dalian 116024, China

Supporting Information

ABSTRACT: Two novel lanthanide complex-based luminescent probes, ANMTTA-Eu^{3+} and ANMTTA-Tb^{3+} {ANMTTA, [4′-(4-amino-3-nitrophenoxy)methylene-2,2′:6′,2″-terpyridine-6,6″-diyl] bis(methylenenitrilo) tetrakis(acetic acid)}, have been designed and synthesized for the highly sensitive and selective time-gated luminescence detection of hypochlorous acid (HOCl) in aqueous media. The probes are almost nonluminescent due to the photoinduced electron transfer (PET) process from the 4-amino-3-nitrophenyl moiety to the terpyridine-Ln^{3+} moiety, which quenches the lanthanide luminescence effectively. Upon reaction with HOCl, the 4-amino-3-nitrophenyl moiety is rapidly cleaved from the probe complexes, which affords strongly luminescent lanthanide complexes HTTA-Eu^{3+} and HTTA-Tb^{3+} {HTTA, (4′-hydroxymethyl-2,2′:6′,2″-terpyridine-6,6″-diyl) bis(methylenenitrilo) tetrakis(acetic acid)}, accompanied by the remarkable luminescence enhancements. The dose-dependent luminescence enhancements show good linearity with detection limits of 1.3 nM and 0.64 nM for HOCl with ANMTTA-Eu^{3+} and ANMTTA-Tb^{3+}, respectively. In addition, the luminescence responses of ANMTTA-Eu^{3+} and ANMTTA-Tb^{3+} to HOCl are pH-independent with excellent selectivity to distinguish HOCl from other reactive oxygen/nitrogen species (ROS/RNS). The ANMTTA-Ln^{3+}-loaded HeLa and RAW 264.7 macrophage cells were prepared, and then the exogenous HOCl in HeLa cells and endogenous HOCl in macrophage cells were successfully imaged with time-gated luminescence mode. The results demonstrated the practical applicability of the probes for the cell imaging application.

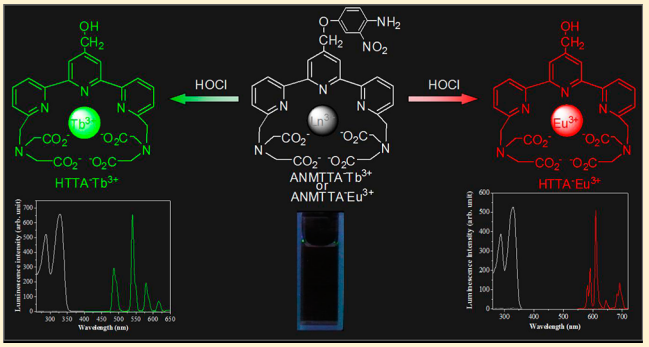

Hypochlorous acid (HOCl) is one of the weakly acidic reactive oxygen species (ROS) and partially dissociates into hypochlorite anion in the physiological pH solution.[1,2] In a certain concentration range, HOCl can serve as a potent bactericide due to its strong oxidizability[1] and is widely employed as a bleaching agent in our daily life.[2] On the other hand, HOCl is also one of the normal byproducts of cellular metabolism and plays pivotal roles in many biological vital processes.[3,4] In organisms, HOCl can be synthesized via the reaction of hydrogen peroxide and chloride anion catalyzed by myeloperoxidase (MPO), which is mainly stored in azurophilic granules of leukocytes (including neutrophils, macrophages, and monocytes).[5,6] MPO is a heme-containing enzyme that can be released by inflammatory mediators such as neutrophils and macrophages stimulated by lipopolysaccharide (LPS) and 4β-phorbol-12-myristate-13-acetate (PMA).[7−9] Despite important functions of HOCl in microorganism invasion,[10] the excess generation of HOCl can lead to inflammation-associated tissue injury, such as hepatic ischemiareperfusion injury,[11] atherosclerosis,[12] lung injury,[13] and rheumatoid arthritis.[14] To date, detailed investigations of the oxidation biology of HOCl were hampered in part owing to the difficulty in tracking such a small reactive oxygen metabolite in real time, especially in live-cell settings, which motivates researchers to develop sensitive and selective probes for the monitoring of HOCl, to supply accurate and reliable HOCl signals both *in vivo* and *in vitro*.

In recent several years, some fluorescent probes and materials have been reported for the detection of HOCl.[15−25] Most of them were developed on the basis of the conjugation of an organic fluorophore with a HOCl-recognizing moiety, such as *p*-methoxyphenol,[26] thiol,[27−29] dibenzoylhydrazine,[30,31] hydroxamic acid,[32] and oxim derivatives.[33,34] Although these organic dye-based probes can quantify HOCl concentrations in biological samples with changes in fluorescence intensity, the detection is often hampered by the background fluorescence derived from the endogenous components of biological samples, such as flavins, nicotinamide adenine dinucleotides, and porphyrins.[35,36] To enhance the sensing sensitivity of fluorescence probes for the real-time monitoring of HOCl in complicated biological samples, a more efficient approach is the time-gated luminescence measurement technique using lanthanide complexes as probes.[37−40] In comparison to the short-lived fluorescence of organic probes, the luminescence of lanthanide(III) (mainly Eu^{3+} and Tb^{3+}) complex probes is long-

Received: September 28, 2012
Accepted: November 28, 2012
Published: November 28, 2012

   dx.doi.org/10.1021/ac3028189 | *Anal. Chem.* 2012, 84, 10785−10792

Scheme 1. Reaction Mechanism of the Luminescence Response of ANMTTA-Ln^{3+} Towards HOCl

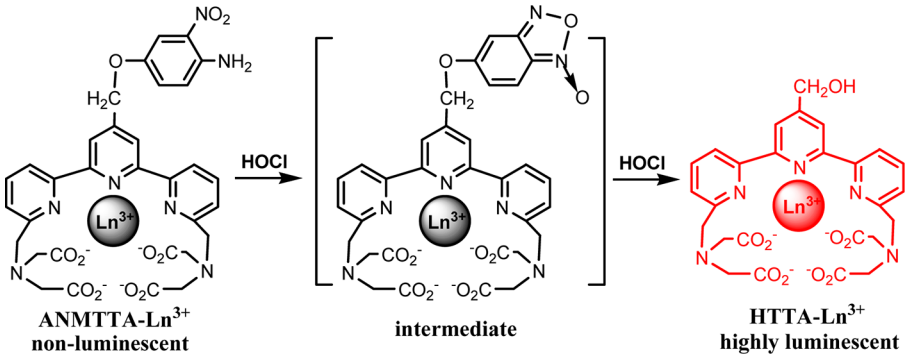

lived with large Stokes shifts and sharp emission profiles, which enables these complexes to be easily used for the time-gated luminescence measurement to eliminate the interferences from autofluorescence and scattering lights.[41,42] Recently, on the basis of successful designs and syntheses of some dual-functional ligands, lanthanide complex-based luminescent probes that can specifically respond to small bioactive molecules and ions, such as singlet oxygen, $ONOO^-$, NO, H_2O_2, uric acid, K^+, Zn^{2+}, and a number of anions, have been developed.[43−53] These probes exhibited high sensitivities for the time-gated luminescence detections of bioactive targets. Nevertheless, little attention has been paid to develop such kind of probes for the selective and sensitive detection of HOCl in biological samples.

In a quite recent work we found that the lanthanide (Eu^{3+} and Tb^{3+}) complexes with [4′-(*p*-aminophenoxy)methylene-2,2′:6′,2″-terpyridine-6,6″-diyl] bis(methylenenitrilo) tetrakis-(acetate) (AMTTA-Ln^{3+}) could be used as efficient luminescence probes for the time-gated luminescence detection of highly reactive oxygen species (HOCl and $^{\bullet}OH$).[54] Because AMTTA-Ln^{3+} lacks the recognition specificity to distinguish HOCl and $^{\bullet}OH$ radicals, in this work, a novel dual-functional chelating ligand that can strongly coordinate with both Eu^{3+} and Tb^{3+} for specifically recognizing HOCl in aqueous media, [4′-(4-amino-3-nitrophenoxy)methylene-2,2′:6′,2″-terpyridine-6,6″-diyl] bis(methylenenitrilo) tetrakis(acetic acid) (ANMTTA), was designed and synthesized. Because of the photo-induced electron transfer (PET) from the *o*-nitroanilino group to the terpyridine-Ln^{3+} moiety, the complexes ANMTTA-Eu^{3+} and ANMTTA-Tb^{3+} are almost nonluminescent. However, in the presence of HOCl, the specific reaction between the *o*-nitroanilino group and HOCl triggers the cleavage of the 4-amino-3-nitrophenyl ether in the complexes, eliminating the PET process so that the luminescence of on-state complexes, (4′-hydroxymethyl-2,2′:6′,2″-terpyridine-6,6″-diyl) bis-(methylenenitrilo) tetrakis(acetate)-Ln^{3+} (HTTA-Ln^{3+}), is turned on. On the basis of this specific response, a highly selective and sensitive time-gated luminescence detection method for HOCl using ANMTTA-Ln^{3+} as probes was established. To examine the potential of new probes for cell imaging application, the cell-membrane permeable complexes, the acetoxymethyl ester of ANMTTA-Ln^{3+} (AM-ANMTTA-Ln^{3+}),[55,56] were further synthesized for loading the complexes into living cells. In combination with a time-gated luminescence microscope, the exogenous and endogenous HOCl in HeLa and RAW 264.7 macrophage cells were successfully monitored, respectively. Scheme 1 shows the reaction mechanism of the luminescence response of ANMTTA-Ln^{3+} toward HOCl.

EXPERIMENTAL SECTION

Materials and Physical Measurements. Tetraethyl (4′-bromomethyl-2,2′:6′,2″- terpyridine-6,6″-diyl) bis-(methylenenitrilo) tetrakis(acetate) (compound **1**) and (4′-hydroxymethyl-2,2′:6′,2″-terpyridine-6,6″-diyl) bis-(methylenenitrilo) tetrakis(acetic acid) (HTTA) were synthesized according to the previous method.[54] 4-Amino-3-nitrophenol was purchased from Acros Organics. Tetrahydrofuran (THF) and acetonitrile were used after appropriate distillation and purification. 4*β*-Phorbol-12-myristate-13-acetate (PMA), lipopolysaccharide (LPS), and interferon-*γ* (IFN-*γ*) were purchased from Sigma-Aldrich. The cultured HeLa and RAW 264.7 macrophage cells were obtained from Dalian Medicine University. A stock solution of hypochlorite was prepared from the commercial sodium hypochlorite solution and stored according to the literature method.[57] The concentration was determined by using its molar extinction coefficient of 391 M^{-1} cm^{-1} at 292 nm before use.[57] Unless otherwise specified, all chemical materials were purchased from commercial sources and used without further purification. The deionized distilled water was used throughout.

^1H and ^{13}C NMR spectra were recorded on a Bruker Avance spectrometer (400 MHz for ^1H and 100 MHz for ^{13}C). Mass spectra were measured on a HP1100LC/MSD electrospray ionization mass spectrometer (ESI-MS). Elemental analysis was carried out on a Vario-EL CHN analyzer. Time-gated luminescence spectra and luminescence properties were measured on a Perkin-Elmer LS 50B luminescence spectrometer with the settings of excitation wavelength, 330 nm; delay time, 0.2 ms; gate time, 0.4 ms; cycle time, 20 ms; excitation slit, 10 nm; and emission slit, 5 nm. The luminescence quantum yields (ϕ) of ANMTTA-Eu^{3+}, ANMTTA-Tb^{3+}, HTTA-Eu^{3+}, and HTTA-Tb^{3+} were measured by using the previous methods.[43,44] The calibration curves for the time-gated luminescence detection of HOCl using ANMTTA-Eu^{3+} and ANMTTA-Tb^{3+} as probes were measured on a Perkin-Elmer Victor 1420 multilabel counter with the settings of excitation wavelength, 330 nm; delay time, 0.2 ms; counting time, 0.4 ms; and cycling time, 1.0 ms. All bright-field, steady-state, and time-gated luminescence imaging measurements were carried out on a laboratory-use luminescence microscope (see the Supporting Information).[43]

Synthesis of ANMTTA. The reaction pathway for the synthesis of the new ligand ANMTTA is shown in Scheme S1 in the Supporting Information. The details are described as follows.

Synthesis of Tetraethyl [4′-(4-amino-3-nitrophenoxy)-methylene-2,2′:6′,2″-terpyridine-6,6″-diyl] Bis-

dx.doi.org/10.1021/ac3028189 | *Anal. Chem.* 2012, 84, 10785−10792

(methylenenitrilo) Tetrakis(acetate) (Compound 2). A mixture of 4-amino-3-nitrophenol (203 mg, 1.32 mmol) and NaH (31.7 mg, 1.32 mmol) in 20 mL of dry acetonitrile was stirred at room temperature for 15 min under an argon atmosphere, then compound **1** (320 mg, 0.44 mmol) was added. The suspension was further stirred overnight under an argon atmosphere. After filtration, the solvent was evaporated. Purification by silica gel column chromatography with CH_2Cl_2/CH_3OH (20:1, v/v) as eluent gave the compound **2** as a red oil (200 mg, 56.7% yield). ^{1}H NMR (400 MHz, $CDCl_3$): δ = 1.24 (t, J = 8.0 Hz, 12H), 3.70 (s, 8H), 4.15−4.21 (m, 12H), 5.18 (s, 2H), 6.85 (d, J = 8.0 Hz, 1H), 7.23 (dd, J = 8.0 Hz, 1H), 7.63 (d, J = 8.0 Hz, 2H), 7.67 (d, J = 8.0 Hz, 1H), 7.84 (t, J = 8.0 Hz, 2H), 8.49 (s, 2H), 8.51 (s, 2H). ^{13}C NMR (100 MHz, $CDCl_3$): δ = 14.23, 54.92, 59.94, 60.59, 69.33, 107.53, 118.95, 119.79, 120.43, 123.34, 127.23, 130.88, 137.63, 140.86, 147.29, 149.13, 155.05, 155.70, 158.22, 171.27. ESI-MS (m/z): 802.2 ([M + H]$^+$).

Synthesis of ANMTTA. A mixture of compound **2** (200 mg, 0.25 mmol), KOH (390 mg, 7 mmol), 1.0 mL of water, and 11 mL of ethanol was stirred at room temperature for 20 h. After evaporation, the residue was dissolved in 3 mL of water, and the solution was acidized to pH ∼3 with HCl (3 M). The suspension was stirred for another 20 h at room temperature, and then the precipitate was collected by filtration. After drying, the precipitate was added to 30 mL of dry acetonitrile, and the mixture was refluxed for 30 min. The precipitate was filtered and dried again to afford ANMTTA as a yellow solid (165 mg, 95.8% yield). ^{1}H NMR (400 MHz, DMSO-d_6): δ = 3.56 (s, 8H), 4.10 (s, 4H), 5.35 (s, 2H), 7.04 (d, J = 8.0 Hz, 1H), 7.32 (s, 2H), 7.37 (dd, J = 8.0 Hz, 1H), 7.58 (d, J = 8.0 Hz, 1H), 7.65 (d, J = 8.0 Hz, 2H), 7.99 (t, J = 8.0 Hz, 2H), 8.49 (s, 2H), 8.51 (d, J = 8.0 Hz, 2H). ^{13}C NMR (100 MHz, DMSO-d_6): δ = 54.85, 59.75, 69.05, 107.23, 118.95, 119.79, 121.34, 123.75, 128.15, 129.52, 138.39, 142.71, 148.28, 148.85, 154.65, 155.58, 159.37, 172.89. ESI-MS (m/z): 688.3 ([M − H]$^-$). Elemental analysis calcd (%) for $C_{32}H_{31}N_7O_{11}\cdot 3H_2O$ (ANMTTA·3H_2O): C 51.68, H 5.01, N 13.18; found (%) C 51.51, H 4.68, N 13.05.

Syntheses of Ln^{3+} Complexes. ANMTTA·3H_2O (4.0 mg, 5.44 μmol) and $TbCl_3\cdot 6H_2O$ (2.0 mg, 5.44 μmol) were added to 1.36 mL of 50 mM borate buffer of pH 7.4. After the mixture was stirred at room temperature for 0.5 h, the obtained stock solution of ANMTTA-Tb^{3+} (4.0 mM) was stored at −20 °C and suitably diluted with aqueous buffers before use. The stock solutions of the complexes ANMTTA-Eu^{3+}, HTTA-Tb^{3+}, and HTTA-Eu^{3+} were prepared with the same method.

Synthesis of AM-ANMTTA-Ln^{3+}. A solution of ANMTTA·3H_2O (11.5 mg, 15.5 μmol), triethylamine (22 μL, 155 μmol), and bromomethyl acetate (61 μL, 618 μmol) in anhydrous dimethyl sulfoxide (227 μL) was stirred at room temperature for 48 h. After the precipitate was removed by centrifugation, the supernatant (AM-ANMTTA concentration, ∼50 mM) was collected carefully and characterized by mass spectrometry. ESI-MS (m/z): 998.8 [M − 2H$^+$ + Na$^+$]$^-$. To the solution was added $LnCl_3\cdot 6H_2O$ (final concentration, 50 mM; Ln, Eu, or Tb), and then the solution was stirred for another 0.5 h. The freshly prepared stock solution of AM-ANMTTA-Ln^{3+} (50 mM) was used for the cell loading without further purification.[44]

Cell Culture and Imaging. Two kinds of cultured cells, HeLa and RAW 264.7 macrophage cells, were used for the luminescence imaging measurements. The experimental details are described as follows.

HeLa Cells. HeLa cells were cultured in RPMI-1640 medium (Sigma-Aldrich), supplemented with 10% fetal bovine serum (Corning Inc.), 1% penicillin (Gibco), and 1% streptomycin (Gibco) at 37 °C in a 5% CO_2/95% air incubator. For detection of intracellular HOCl, the cultured HeLa cells in a T-75 flask were washed three times with Krebs-Ringer phosphate buffer (KRP buffer, 114 mM NaCl, 4.6 mM KCl, 2.4 mM $MgSO_4$, 1.0 mM $CaCl_2$, 15 mM Na_2HPO_4/NaH_2PO_4, pH 7.4) and then incubated with the KRP buffer containing 500 μM of AM-ANMTTA-Eu^{3+} for 4 h at 37 °C in a 5% CO_2/95% air incubator. After washing three times with KRP buffer, the cells were cultured for another 30 min with the KRP buffer containing 10 μM, 15 μM, and 20 μM of HOCl, respectively. The cells were washed five times carefully with KRP buffer and then subjected to the luminescence imaging measurement.

RAW 264.7 Macrophage Cells. The macrophage cells were cultured in DMEM medium (Sigma-Aldrich), supplemented with 10% fetal bovine serum (Corning Inc.), 1% penicillin (Gibco), and 1% streptomycin (Gibco) at 37 °C in a 5% CO_2/95% air incubator. Before loading with the luminescent probe, the cells in a T-75 flask were stimulated by LPS and IFN-γ (1.0 μg/mL for LPS, 50 ng/mL for IFN-γ) for 4 h in the culture medium. After washing three times with KRP buffer, the cells were incubated with the KRP buffer containing 500 μM of AM-ANMTTA-Ln^{3+} for 2.5 h in the incubator. The cells were washed three times and then incubated with the KRP buffer containing 1.0 μg/mL of PMA for another 1 h. The cells were rinsed three times with KRP buffer, and then their luminescence images were recorded.

To confirm that the luminescence signals from the cells were originated from the reaction of the probe with the endogenous intracellular HOCl, a control experiment was carried out by incubating the ANMTTA-Ln^{3+}-loaded cells with the KRP buffer containing 2.0 μM of 4-aminobenzoic acid hydrazide (a MPO inhibitor).[58] After incubation for 15 min, 1.0 μg/mL of PMA was added and the cells were incubated for another 1 h. The cells were rinsed three times with KRP buffer, and then their luminescence images were recorded again.

RESULTS AND DISCUSSION

Design and Characterization of the Probes. In recent several years, the strategy of ligand-modulated lanthanide luminescence with PET mechanism by incorporating an electron-rich molecular recognition group into luminescent lanthanide complexes has been demonstrated to be a useful tool for the design of lanthanide complex-based target-responsive luminescent probes.[45,46,56] To design time-gated luminescence probes specific for HOCl, in this work, we chose the Ln^{3+} (Eu^{3+} or Tb^{3+}) complex with (2,2′:6′,2″-terpyridine-6,6″-diyl) bis-(methylenenitrilo) tetrakis(acetate) as a luminophore owing to its high luminescence quantum yield, stability, and solubility in aqueous media, and introduced an unprecedented 4-amino-3-nitrophenyloxy moiety into the complex's ligand to specifically recognize HOCl. Because of the PET process from the 4-amino-3-nitrophenyl moiety to terpyridine moiety, the intramolecular energy transfer from the antenna to the central Ln^{3+} ion is no longer existent, so that the Ln^{3+} luminescence is efficiently quenched. However, in the presence of HOCl, the 4-amino-3-nitrophenyl moiety of the complex can be oxidized by one HOCl to generate a intermediate of benzofurazan-1-oxide (BFO) derivative,[59,60] and such an intermediate is unstable and can be further oxidized by another HOCl to afford a highly

dx.doi.org/10.1021/ac3028189 | Anal. Chem. 2012, 84, 10785−10792

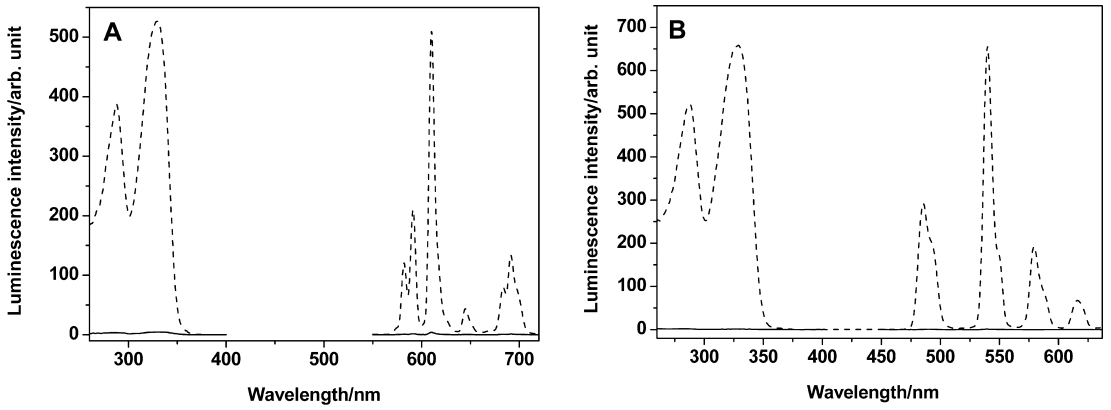

Figure 1. Time-gated excitation and emission spectra of ANMTTA-Eu^{3+} (A, 5.0 μM) and ANMTTA-Tb^{3+} (B, 2.0 μM) in the absence (solid lines) and presence (dashed lines) of HOCl in 50 mM borate buffer of pH 7.4.

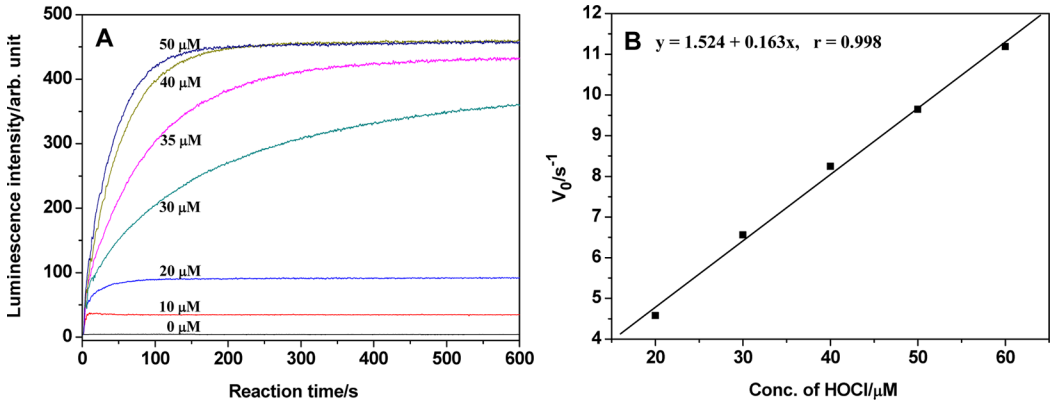

Figure 2. (A) Luminescence response kinetic curves of ANMTTA-Eu^{3+} (5.0 μM) to different concentrations of HOCl in 50 mM borate buffer of pH 7.4. (B) The plot of initial rates (V_0) of the ANMTTA-Eu^{3+}-HOCl reaction against the HOCl concentrations.

luminescent complex HTTA-Ln^{3+} in aqueous media (Scheme 1).[54]

On the basis of the above opinion, the new dual-functional ligand ANMTTA was designed and synthesized according to the reaction pathway as shown in Scheme S1 in the Supporting Information. This ligand was synthesized with two-step reactions using tetraethyl (4′-bromomethyl-2,2′:6′,2″-terpyridine-6,6″-diyl) bis(methylenenitrilo) tetrakis(acetate) (compound **1**) as a starting material. At first, tetraethyl [4′-(4-amino-3-nitrophenoxy)methylene-2,2′:6′,2″-terpyridine-6,6″-diyl] bis(methylenenitrilo) tetrakis(acetate) (compound **2**) was synthesized by reacting compound **1** with 4-amino-3-nitrophenol in anhydrous CH_3CN in the presence of NaH. After the hydrolysis and neutralization of compound **2** with KOH–ethanol–H_2O and HCl, respectively, ANMTTA was obtained with a high yield and well characterized by NMR, ESI-MS, and CHN elementary analyses.

To investigate the luminescence property changes of the lanthanide complexes in the absence and presence of HOCl, the solutions of ANMTTA-Eu^{3+} and ANMTTA-Tb^{3+} were prepared by mixing ANMTTA with 1.0 molar equiv of $LnCl_3$ in 50 mM borate buffer of pH 7.4,[54] and then their absorption and time-gated luminescence spectra in the absence and presence of HOCl were measured. As shown in Figure 1, both ANMTTA-Eu^{3+} and ANMTTA-Tb^{3+} exhibited the same maximum absorption wavelength at 330 nm (ε = 1.46 × 10^4 M^{-1} cm^{-1} and 1.56 × 10^4 M^{-1} cm^{-1} for ANMTTA-Eu^{3+} and ANMTTA-Tb^{3+}, respectively), with very weak emissions centered at 610 nm (ϕ = 0.23%) and 540 nm (ϕ = 0.07%), respectively. However, the addition of HOCl resulted in the remarkable increases in red and green luminescence for ANMTTA-Eu^{3+} and ANMTTA-Tb^{3+}, respectively. Absorption and emission spectra, along with the mass spectrometry data (Figure S1 in the Supporting Information), confirmed that HTTA-Eu^{3+} and HTTA-Tb^{3+}, as the luminescent products, were produced by the HOCl-mediated cleavage of ANMTTA-Eu^{3+} and ANMTTA-Tb^{3+}. Compared to the weak luminescence of ANMTTA-Eu^{3+} and ANMTTA-Tb^{3+}, HTTA-Eu^{3+}, and HTTA-Tb^{3+} showed 71-fold and 164-fold increases in luminescence quantum yields with long luminescence lifetimes (ϕ =16.3% and 11.5% and τ = 1.38 and 1.22 ms for HTTA-Eu^{3+} and HTTA-Tb^{3+}, respectively)[54] in the buffer.

Time-Gated Luminescence Detection of HOCl Using ANMTTA-Ln^{3+} As Probes. To investigate the luminescence response properties of ANMTTA-Ln^{3+} to HOCl, at first, the temporal dynamics of the luminescence response of ANMTTA-Eu^{3+} (5.0 μM) to the additions of different concentrations of HOCl were determined in 50 mM borate buffer of pH 7.4. As shown in Figure 2A, upon the addition of HOCl, a rapid increase in luminescence intensity was observed in a few seconds. After ~200 s reaction, the luminescence intensity reached a plateau and remained stable afterward. By plotting the initial reaction rate (V_0) against the HOCl concentration, a good linearity was obtained with a slope of 1.6 × 10^{-1} s^{-1} μM^{-1} (Figure 2B). Thus, the total reaction rate constant (k_{tot} = slope/C_{probe}) of the ANMTTA-Eu^{3+}-HOCl reaction in the

dx.doi.org/10.1021/ac3028189 | Anal. Chem. 2012, 84, 10785–10792

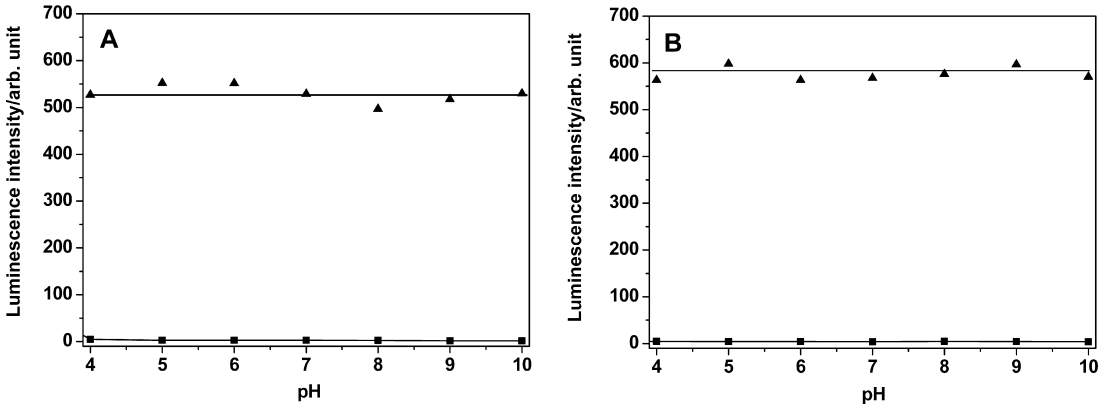

Figure 3. Effects of pH on the time-gated luminescence intensities of (A) ANMTTA-Eu^{3+} (■, 5.0 μM) and HTTA-Eu^{3+} (▲, 5.0 μM) as well as (B) ANMTTA-Tb^{3+} (■, 2.0 μM) and HTTA-Tb^{3+} (▲, 2.0 μM) in 50 mM borate buffers with different pHs.

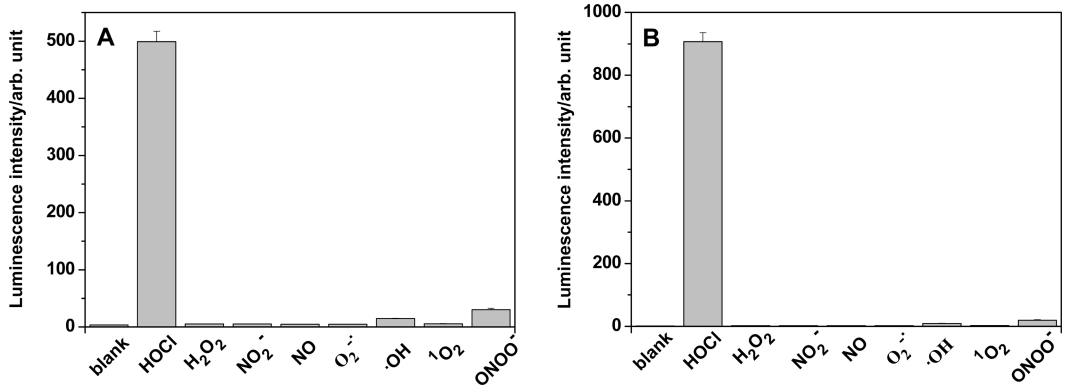

Figure 4. Time-gated luminescence intensities of the products of ANMTTA-Eu^{3+} (A, 5.0 μM) and ANMTTA-Tb^{3+} (B, 5.0 μM) reacted with various ROS/RNS (60 μM) in 50 mM borate buffer of pH 7.4.

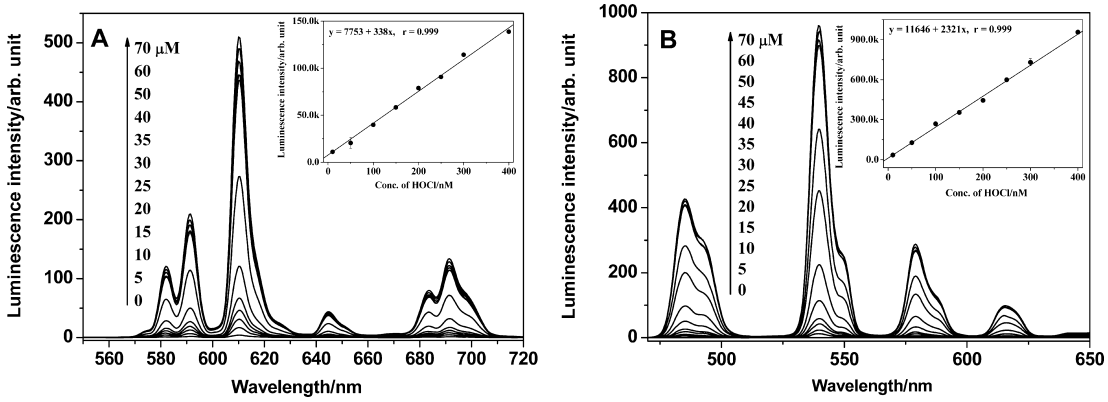

Figure 5. Time-gated emission spectra of ANMTTA-Eu^{3+} (A, 5.0 μM) and ANMTTA-Tb^{3+} (B, 5.0 μM) in the presence of different concentrations of HOCl in 50 mM borate buffer of pH 7.4. λ_{ex} = 330 nm. The insets show the calibration curves for HOCl detection.

buffer was calculated to be 3.3×10^{10} s^{-1} M^{-2} (almost the same result of $k_{tot} = 2.9 \times 10^{10}$ s^{-1} M^{-2} was also obtained from the ANMTTA-Tb^{3+}-HOCl reaction). These results indicate that the luminescence response of ANMTTA-Ln^{3+} to HOCl is very rapid, which is favorable for the detection of HOCl in complicated biosystems.

The Job's plotting analysis of the reaction between ANMTTA-Ln^{3+} and HOCl was conducted in the borate buffer to investigate the stoichiometry of the reaction. As shown in Figure S2 in the Supporting Information, both for the reactions of ANMTTA-Eu^{3+}-HOCl and ANMTTA-Tb^{3+}-HOCl, the maximum luminescence intensities were achieved at ~0.66 molecular fractions, which indicates that the reaction between ANMTTA-Ln^{3+} and HOCl has a 1:2 stoichiometry, corresponding to the reaction mechanism that is shown in Scheme 1. Moreover, the effects of pH on the luminescence intensities of ANMTTA-Ln^{3+} and HTTA-Ln^{3+} were measured in 50 mM borate buffers with different pHs. As shown in Figure 3, the luminescence intensities of ANMTTA-Ln^{3+} and their reaction products with HOCl, HTTA-Ln^{3+}, are all pH-independent in the range of pH 4.0−10, indicating that ANMTTA-Eu^{3+} and ANMTTA-Tb^{3+} can be used as luminescent probes for HOCl detection in weakly acidic, neutral, and basic media.

dx.doi.org/10.1021/ac3028189 | *Anal. Chem.* 2012, 84, 10785−10792

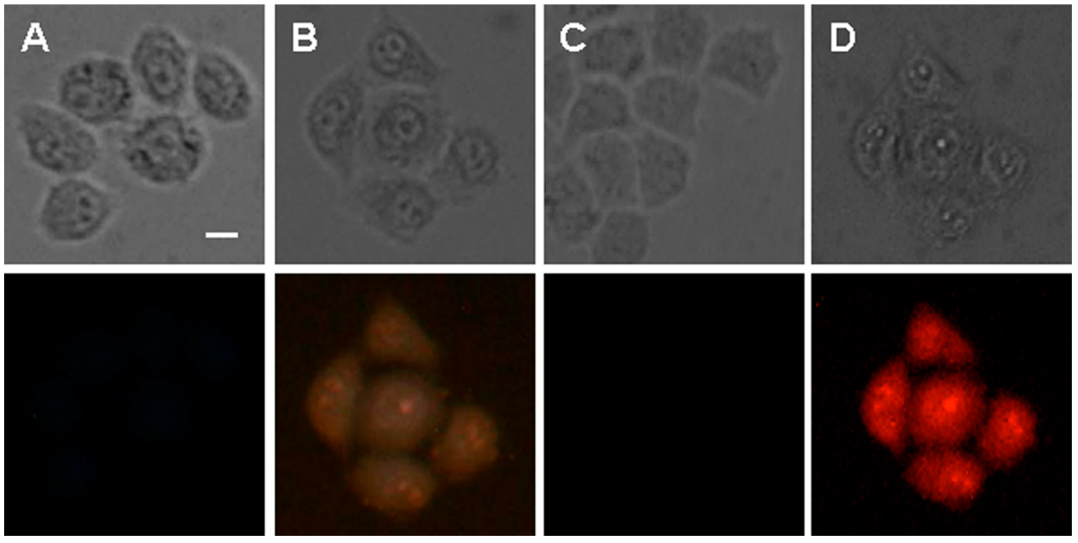

Figure 6. Steady-state (A, B) and time-gated (C, D) luminescence images of the ANMTTA-Eu^{3+}-loaded HeLa cells before (A, C) and after (B, D) incubation with 15 μM HOCl. Scale bar: 10 μm.

To investigate the luminescence response specificity of ANMTTA-Ln^{3+} to HOCl, the reactions of ANMTTA-Ln^{3+} with different ROS/RNS were examined in 50 mM borate buffer of pH 7.4. As shown in Figure 4, ANMTTA-Eu^{3+} and ANMTTA-Tb^{3+} did not give any observable luminescence responses to the additions of $^{\bullet}OH$, NO, H_2O_2, NO_2^-, $ONOO^-$, $^1O_2$, and $O_2^{\bullet-}$, while the luminescence intensities were remarkably increased after ANMTTA-Eu^{3+} and ANMTTA-Tb^{3+} were reacted with HOCl. These results demonstrate that the luminescence responses of the two lanthanide complexes to HOCl are highly specific without the interferences of other ROS/RNS.

On the basis of the above results, the time-gated luminescence titration experiments of HOCl using ANMTTA-Eu^{3+} and ANMTTA-Tb^{3+} as probes were conducted in 50 mM borate buffer of pH 7.4. Figure 5 shows the luminescence titration results where different concentrations of HOCl were added into the solutions of ANMTTA-Eu^{3+} (5.0 μM) and ANMTTA-Tb^{3+} (5.0 μM), respectively. Upon the addition of HOCl, the luminescence intensities of ANMTTA-Eu^{3+} and ANMTTA-Tb^{3+} were significantly increased with up to 100-fold and 600-fold luminescence enhancements. More importantly, the emission intensities of the two complexes showed good linear correlations with the HOCl concentration in the range of 10^{-8} to 10^{-6} M (the insets in Figure 5). The detection limits, calculated according to the reported method defined by IUPAC,[61] are 1.3 nM and 0.64 nM for HOCl with ANMTTA-Eu^{3+} and ANMTTA-Tb^{3+}, respectively. These results reveal that the two complexes are all useful for the sensitive time-gated luminescence detection of HOCl and in which ANMTTA-Tb^{3+} undergoes the greatest absolute change in luminescence turn-on upon reaction with HOCl compared to other reported probes.[62]

Luminescence Imaging of Exogenous HOCl in HeLa Cells. To evaluate the applicability of ANMTTA-Ln^{3+} for imaging HOCl in living cells, according to the previous method,[44,45] the acetoxymethyl ester of ANMTTA-Ln^{3+} (AM-ANMTTA-Ln^{3+}) was synthesized for preparing the ANMTTA-Ln^{3+}-loaded cells because it could be easily transferred into the cells with an ordinary incubation method, and in the cells, accompanied by the rapid hydrolysis of the acetoxymethyl ester of the ligand catalyzed by ubiquitous intracellular esterases, the probe complex ANMTTA-Ln^{3+} could be regenerated.

After the cultured HeLa cells were incubated with the KRP buffer containing 500 μM of AM-ANMTTA-Ln^{3+} for 4 h at 37 °C in a 5% CO_2/95% air incubator, the ANMTTA-Ln^{3+}-loaded HeLa cells were prepared and used for the luminescent imaging of exogenous HOCl. As shown in Figure 6 and Figures S3 and S4 in the Supporting Information, the ANMTTA-Ln^{3+}-loaded cells only emitted weak background blue fluorescence and no time-gated luminescence from the cells could be observed. After the cells were incubated with HOCl for another 30 min, wine steady-state luminescence (mixed color of blue and red from the cell components and the Eu^{3+} complex) and red time-gated luminescence from the ANMTTA-Eu^{3+}-loaded cells (Figure 6 and Figure S3 in the Supporting Information), and bright cyan steady-state luminescence (mixed color of blue and green from cell components and the Tb^{3+} complex) and green time-gated luminescence from the ANMTTA-Tb^{3+}-loaded cells (Figure S4 in the Supporting Information), were clearly observed. These results indicate that ANMTTA-Ln^{3+} has been transferred into the cells and can react with the intracellular HOCl molecules to give the specific and long-lived luminescence signals of the Eu^{3+} and Tb^{3+} complexes.

Luminescence Imaging of Endogenous HOCl in RAW 264.7 Macrophages. The results of the above exogenous HOCl imaging motivated us to further evaluate the feasibility of ANMTTA-Ln^{3+} for the time-gated luminescence imaging of endogenous HOCl generation in macrophage cells. It is known that, upon the stimulation of LPS/IFN-γ/PMA, macrophage cells can release MPO,[8] which rapidly consumes H_2O_2 to form HOCl.[63,64] Thus, after the RAW 264.7 macrophage cells were incubated with LPS/IFN-γ, AM-ANMTTA-Ln^{3+}, and PMA (a known activator of the cells respiratory burst to give rise to ROS)[9,65] for 4, 2.5, and 1 h, respectively, the time-gated luminescence images of the cells were recorded. As shown in Figure 7 and Figure S5 in the Supporting Information, the ANMTTA-Eu^{3+}- and ANMTTA-Tb^{3+}-loaded macrophage cells emitted clearly red and green luminescence, whereas the cells that incubated with 4-aminobenzoic acid hydrazide and then with PMA in the control experiment were almost non-luminescent. The quantitative analysis of the images of the

dx.doi.org/10.1021/ac3028189 | *Anal. Chem.* 2012, 84, 10785−10792

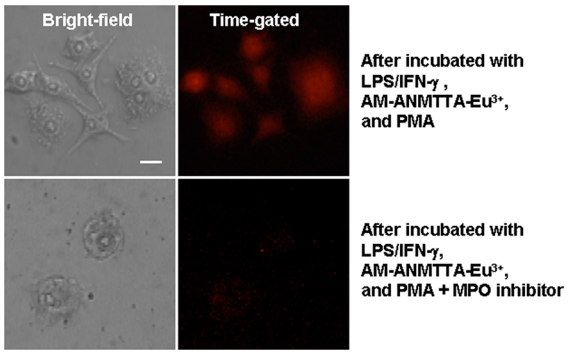

Figure 7. Time-gated luminescence images of the ANMTTA-Eu^{3+}-loaded RAW 264.7 macrophage cells after stimulation with LPS/IFN-γ/PMA (top) or stimulated with LPS/IFN-γ/PMA/4-aminobenzoic acid hydrazide (bottom). Scale bar: 10 μm.

ANMTTA-Eu^{3+}-loaded macrophage cells revealed that the time-gated luminescence intensity from the cells was ~5.8-fold increased after the stimulation (Figure S6 in the Supporting Information). These results indicate that HOCl was generated in the LPS/IFN-γ/PMA-stimulated RAW 264.7 macrophage cells and was indeed visualized by using ANMTTA-Eu^{3+} as a probe.

The cytotoxicities of the two probes to RAW264.7 macrophage cells were measured with the MTT assay method. As shown in Figure S7 in the Supporting Information, the cell viabilities remained still above 90% after incubation with 250 μM, 500 μM, and 700 μM of AM-ANMTTA-Ln^{3+} for 2.5 h. These results indicate that the toxicity of the probe is low to the cultured cells.

CONCLUSIONS

In this work we have successfully developed two lanthanide complex-based luminescent probes, ANMTTA-Eu^{3+} and ANMTTA-Tb^{3+}, for the recognition and time-gated luminescence detection of HOCl in aqueous media. The new probes were designed and synthesized with the PET mechanism by incorporating a HOCl-specific recognition moiety, 4-amino-3-nitrophenyl, into the lanthanide complexes of terpyridine polyacid ligand. The almost nonluminescent probes can react with HOCl under physiological conditions to yield highly luminescent products, HTTA-Eu^{3+} and HTTA-Tb^{3+}, with remarkable luminescence enhancements. Compared to the previously reported luminescent probes for HOCl, the new probes possess several desirable properties including large Stokes shift, sharp emission profile, high water-solubility, selectivity, and reaction rate, and pH-independent luminescence response behavior. Moreover, the long-lived luminescence of the probes and their HOCl-reaction products allows the probes to be favorably useful for the background-free time-gated luminescence detection of HOCl in complicated biological samples. The preliminary results shown here of time-gated luminescence imaging to monitor the exogenous and endogenous HOCl in living cells demonstrated the applicability of the probes for the *in vivo* HOCl detection, which would be a useful tool for the investigation of biological functions of HOCl in living systems.

ASSOCIATED CONTENT

Supporting Information

Schematic pathway for the synthesis of ANMTTA, the details of luminescence microscopy and cytotoxicity measurements, and supplementary figures. This material is available free of charge via the Internet at http://pubs.acs.org.

AUTHOR INFORMATION

Corresponding Author

*E-mail: zhiqiangye2001@yahoo.com.cn (Z.Y.); jingliyuan@yahoo.com.cn (J.Y.). Phone/fax: +86-411-84986041.

Notes

The authors declare no competing financial interest.

ACKNOWLEDGMENTS

Financial support from the National Natural Science Foundation of China (Grant No. 20835001) is gratefully acknowledged.

REFERENCES

(1) Lapenna, D.; Cuccurullo, F. *Gen. Pharmacol.* **1996**, *27*, 1145–1147.
(2) Aokl, T.; Munemorl, M. *Anal. Chem.* **1983**, *55*, 209–212.
(3) Ozben, T. *J. Pharm. Sci.* **2007**, *96*, 2181–2196.
(4) Winterbourn, C. C. *Nat. Chem. Biol.* **2008**, *4*, 278–286.
(5) Yap, Y. W.; Whiteman, M.; Cheung, N. S. *Cell Signal.* **2007**, *19*, 219–228.
(6) Pattison, D. I.; Davies, M. J. *Biochemistry* **2006**, *45*, 8152–8162.
(7) Daugherty, A.; Dunn, J. L.; Rateri, D. L.; Heinecke, J. W. *J. Clin. Invest.* **1994**, *94*, 437–444.
(8) Muijsers, R. B. R.; van den Worm, E.; Folkerts, G.; Beukelman, C. J.; Koster, A. S.; Postma, D. S.; Nijkamp, F. P. *Br. J. Pharmacol.* **2000**, *130*, 932–936.
(9) Salonen, T.; Sareila, O.; Jalonen, U.; Kankaanranta, H.; Tuominen, R.; Moilanen, E. *Br. J. Pharmacol.* **2006**, *147*, 790–799.
(10) Adam, L. C.; Gordon, G. *Anal. Chem.* **1995**, *67*, 535–540.
(11) Hasegawa, T.; Malle, E.; Farhood, A.; Jaeschke, H. *Am. J. Physiol. Gastrointest. Liver Physiol.* **2005**, *289*, 760–767.
(12) Zhang, R.; Brennan, M. L.; Fu, X.; Aviles, R. J.; Pearce, G. L.; Penn, M. S.; Topol, E. J.; Sprecher, D. L.; Hazen, S. L. *JAMA, J. Am. Med. Assoc.* **2001**, *286*, 2136–2142.
(13) Hammerschmidt, S.; Buchler, N.; Wahn, H. *Chest* **2002**, *121*, 573–581.
(14) Wu, S. M.; Pizzo, S. V. *Arch. Biochem. Biophys.* **2001**, *391*, 119–126.
(15) Dickinson, B. C.; Srikunand, D.; Chang, C. J. *Curr. Opin. Chem. Biol.* **2010**, *14*, 50–56.
(16) Dickinson, B. C.; Chang, C. J. *Nat. Chem. Biol.* **2011**, *7*, 504–511.
(17) Yan, Y.; Wang, S.; Liu, Z.; Wang, H.; Huang, D. *Anal. Chem.* **2010**, *82*, 9775–9781.
(18) Lou, X.; Zhang, Y.; Li, Q.; Qin, J.; Li, Z. *Chem. Commun.* **2011**, *47*, 3189–3191.
(19) Zhao, N.; Wu, Y. H.; Wang, R. M.; Shi, L. X.; Chen, Z. N. *Analyst* **2011**, *136*, 2277–2282.
(20) Chen, S.; Lu, J.; Sun, C.; Ma, H. *Analyst* **2010**, *135*, 577–582.
(21) Huo, F. J.; Zhang, J. J.; Yang, Y. T.; Chao, J. B.; Yin, C. X.; Zhang, Y. B.; Chen, T. G. *Sens. Actuators, B: Chem.* **2012**, *166–167*, 44–49.
(22) Kim, T. I.; Park, S.; Choi, Y.; Kim, Y. *Chem. Asian J.* **2011**, *6*, 1358–1361.
(23) Yuan, L.; Lin, W.; Yang, Y.; Chen, H. *J. Am. Chem. Soc.* **2012**, *134*, 1200–1211.
(24) Shepherd, J.; Hilderbrand, S. A.; Waterman, P.; Heinecke, J. W.; Weissleder, R.; Libby, P. *Chem. Biol.* **2007**, *14*, 1221–1231.

(25) Panizzi, P.; Nahrendorf, M.; Wildgruber, M.; Waterman, P.; Figueiredo, J.; Aikawa, E.; McCarthy, J.; Weissleder, R.; Hilderbrand, S. A. *J. Am. Chem. Soc.* **2009**, *131*, 15739−15744.
(26) Sun, Z. N.; Liu, F. Q.; Chen, Y.; Tam, P. K. H.; Yang, D. *Org. Lett.* **2008**, *10*, 2171−2174.
(27) Kenmoku, S.; Urano, Y.; Kojima, H.; Nagano, T. *J. Am. Chem. Soc.* **2007**, *129*, 7313−7318.
(28) Chen, X.; Lee, K. A.; Ha, E. M.; Lee, K. M.; Seo, Y. Y.; Choi, H. K.; Kim, H. N.; Kim, M. J.; Cho, C. S.; Lee, S. Y.; Lee, W. J.; Yoon, J. *Chem. Commun.* **2011**, *47*, 4373−4375.
(29) Koide, Y.; Urano, Y.; Hanaoka, K.; Terai, T.; Nagano, T. *J. Am. Chem. Soc.* **2011**, *133*, 5680−5682.
(30) Chen, X.; Wang, X.; Wang, S.; Shi, W.; Wang, K.; Ma, H. *Chem.—Eur. J.* **2008**, *14*, 4719−4724.
(31) Yuan, L.; Lin, W.; Song, J.; Yang, Y. *Chem. Commun.* **2011**, *47*, 12691−12693.
(32) Yang, Y. K.; Cho, H. J.; Lee, J.; Shin, I.; Tae, J. *Org. Lett.* **2009**, *11*, 859−861.
(33) Cheng, X.; Jia, H.; Long, T.; Feng, J.; Qin, J.; Li, Z. *Chem. Commun.* **2011**, *47*, 11978−11980.
(34) Lin, W.; Long, L.; Chen, B.; Tan, W. *Chem.—Eur. J.* **2009**, *15*, 2305−2309.
(35) Li, Y.; Wang, H.; Li, J.; Zheng, J.; Xu, X.; Yang, R. *Anal. Chem.* **2011**, *83*, 1268−1274.
(36) Yang, R.; Li, K.; Liu, F.; Li, N.; Zhao, F.; Chan, W. *Anal. Chem.* **2003**, *75*, 3908−3914.
(37) Bunzli, J. C. G. *Chem. Rev.* **2010**, *110*, 2729−2755.
(38) New, E. J.; Parker, D.; Smith, D. G.; Walton, J. W. *Curr. Opin. Chem. Biol.* **2010**, *14*, 238−246.
(39) Thibon, A.; Pierre, V. C. *Anal. Bioanal. Chem.* **2009**, *394*, 107−120.
(40) New, E. J.; Congreve, A.; Parker, D. *Chem. Sci.* **2010**, *1*, 111−118.
(41) Moore, E. G.; Samuel, A. P. S.; Raymond, K. N. *Acc. Chem. Res.* **2009**, *42*, 542−552.
(42) Montgomery, C. P.; Murray, B. S.; New, E J.; Pal, R.; Parker, D. *Acc. Chem. Res.* **2009**, *42*, 925−937.
(43) Song, B.; Wang, G. L.; Tan, M. Q.; Yuan, J. L. *J. Am. Chem. Soc.* **2006**, *128*, 13442−13450.
(44) Song, C. H.; Ye, Z. Q.; Wang, G. L.; Yuan, J. L.; Guan, Y. F. *Chem.—Eur. J.* **2010**, *16*, 6464−6472.
(45) Chen, Y. G.; Guo, W. H.; Ye, Z. Q.; Wang, G. L.; Yuan, J. L. *Chem. Commun.* **2011**, *47*, 6266−6268.
(46) Ye, Z. Q.; Chen, J. X.; Wang, G. L.; Yuan, J. L. *Anal. Chem.* **2011**, *83*, 4163−4169.
(47) Poole, R.; Kielar, F.; Richardson, S. L.; Stenson, P. A.; Parker, D. *Chem. Commun.* **2006**, 4084−4086.
(48) Thibon, A.; Pierre, V. C. *J. Am. Chem. Soc.* **2009**, *131*, 434−435.
(49) Ye, Z. Q.; Wang, G. L.; Chen, J. X.; Fu, X. Y.; Zhang, W. Z.; Yuan, J. L. *Biosens. Bioelectron.* **2010**, *26*, 1043−1048.
(50) Parker, D.; Yu, J. H. *Chem. Commun.* **2005**, 3141−3143.
(51) Leonard, J. P.; Santos, C. M. G.; Plush, S. E.; McCabe, T.; Gunnlaugsson, T. *Chem. Commun.* **2007**, 129−131.
(52) Shao, N.; Jin, J. Y.; Wang, G. L.; Zhang, Y.; Yang, R. H.; Yuan, J. L. *Chem. Commun.* **2008**, 1127−1129.
(53) Tan, C. L.; Wang, Q. M. *Inorg. Chem.* **2011**, *50*, 2953−2956.
(54) Xiao, Y. N.; Ye, Z. Q.; Wang, G. L.; Yuan, J. L. *Inorg. Chem.* **2012**, *51*, 2940−2946.
(55) Tsien, R. Y. *Nature* **1981**, *290*, 527−528.
(56) Koide, Y.; Urano, Y.; Kenmoku, S.; Kojima, H.; Nagano, T. *J. Am. Chem. Soc.* **2007**, *129*, 10324−10325.
(57) Kanofsky, J. R. *J. Org. Chem.* **1986**, *51*, 3386−3388.
(58) Adachi, Y.; Kindzelskii, A. L.; Petty, A. R.; Huang, J. B.; Maeda, N.; Yotsumoto, S.; Aratani, Y.; Ohno, N.; Petty, H. R. *J. Immunol.* **2006**, *176*, 5033−5040.
(59) Mallory, F. B.; Cairns, T. L.; Simmons, H. E. *Org. Synth.* **1963**, *4*, 74−78.
(60) Fäh, H.; Corp, C. G. *Process for producing benzofurazan-1-oxides*. U. S. Patent 4,185,018, January 22, 1980.
(61) Mocak, J.; Bond, A. M.; Mitchell, S.; Scollary, G. *Pure Appl. Chem.* **1997**, *69*, 297−328.
(62) Zhou, Y.; Li, J. Y.; Chu, K. H.; Liu, K.; Yao, C.; Li, J. Y. *Chem. Commun.* **2012**, *48*, 4677−4679.
(63) Rossi, F. *Biochim. Biophys. Acta* **1986**, *853*, 65−89.
(64) Hidalgo, E.; Bartolome, R.; Dominguez, C. *Chem. Biol. Interact.* **2002**, *139*, 265−282.
(65) Repine, J. E.; White, J. G.; Clawson, C. C.; Holmes, B. M. *J. Lab. Clin. Med.* **1974**, *83*, 911−920.